Environment International 157 (2021) 106776

Contents lists available at ScienceDirect

Environment International

journal homepage: www.elsevier.com/locate/envint

Nitrifiers drive successions of particulate organic matter and microbial community composition in a starved macrocosm

Lianbao Zhang [a], Mingming Chen [a], Xiaowei Chen [a], Jianning Wang [a], Yu Zhang [a], Xilin Xiao [a], Chen Hu [a], Jihua Liu [b], Rui Zhang [a], Dapeng Xu [a], Nianzhi Jiao [a], Yao Zhang [a,*]

[a] State Key Laboratory of Marine Environmental Science and College of Ocean and Earth Sciences, Xiamen University, Xiamen 361101, China
[b] Institute of Marine Science and Technology, Shandong University, Qinagdao 266237, China

ARTICLE INFO

Handling Editor: Adrian Covaci

Keywords:
Nitrifiers
Nitrification
Particulate organic matter
Nitrogenous compounds
Aromatic compounds
Starved dark ecosystem

ABSTRACT

Organic carbon produced by nitrifiers plays an important role in maintaining the microbial metabolism in the aphotic ocean layer with carbon and energy scarcity. However, the contribution of nitrifiers to organic carbon processing remains unclear. To explore how nitrification impacts the material cycle in the starved ecosystem, we set up an ultra-large volume, long-term incubation experiment. Seawater collected from the Halifax coastal ocean was pumped into the Aquatron Tower Tank located at Dalhousie University, Canada, and was incubated under dark conditions for 73 days. The results indicated that the relative abundance of nitrifiers increased and nitrification was strengthened in the dark system where energy and organic carbon were scarce. The importance of nitrogenous compounds in particulate materials increased over the course of the incubation. Correlation analysis showed that the relative abundances of nitrifiers and particulate organic compounds containing nitrogen were significantly and positively correlated. Furthermore, network analysis suggested that metabolic processes related to nitrogenous and aromatic compounds are most important to particle associated bacteria. This study suggests that the nitrifiers could produce a series of organic compounds that result in the alteration of organic matter composition by promoting the degradation of recalcitrant aromatic compounds, which has important implications for organic matter processing in the starved dark ecosystem.

1. Introduction

The downward flux of dissolved and particulate organic carbon formed in the photic zone is the major source of carbon supporting heterotrophic respiration in the dark ocean (Arístegui et al., 2002; Arístegui et al., 2009), however this flux can be variable and intermittent (Arístegui and Montero, 2005). Previous studies have indicated that organic carbon transported from surface to the deep ocean did not match microbial carbon demand in the dark ocean (Reinthaler et al., 2006; Baltar et al., 2009; Shen et al., 2020). Recent studies support the idea that organic carbon produced by chemoautotrophs is another important source of organic carbon for microorganisms in the energy and carbon source limiting environment (Reinthaler et al., 2010; Swan et al., 2011).

Many microbial groups have the potential to fix carbon without sunlight, and are supported by various reduced inorganic compounds, including ammonia, sulfide, carbon monoxide, and methane. The predominant types of autotrophy are fueled by ammonia and nitrite oxidization performed by ammonia- and nitrite-oxidizing microorganisms, respectively (Wuchter et al., 2006; Raven, 2009; Pachiadaki et al., 2017; Zhang et al., 2020)). Ammonia-oxidizing archaea (AOA) comprise 20–40% of prokaryotic marine plankton, constituting a significant fraction of microbial biomass (Karner et al., 2001). Previous research has shown that the continuous succession of active microorganisms is driven by nitrifying microorganisms in the starved environment and that the absence of active organic carbon stimulated an increase in the relative abundance of nitrifiers (Sebastián et al., 2018). The fresh organic carbon excreted by nitrifying microorganisms has a priming effect, promoting the degradation of previously unreactive organic matter (Kuzyakov et al., 2000), which then triggers a shift in microbial population composition.

An increase in the relative abundance of pico-sized phytoplankton, caused by global climate change, would reduce the downward flux of organic matter from the surface euphotic layer (Buesseler et al., 2007; Smith et al., 2008). Thus, chemoautotrophic nitrifiers could play an

* Corresponding author.
E-mail address: yaozhang@xmu.edu.cn (Y. Zhang).

https://doi.org/10.1016/j.envint.2021.106776
Received 31 January 2021; Received in revised form 12 July 2021; Accepted 13 July 2021

important role in maintaining the organic carbon-scarce ecosystem. To date, the relationship between nitrifiers and particulate organic matter in the starved ecosystem has been little studied, hindering our understanding of the contribution by nitrifiers to organic matter processing. However, complex natural environments, such as the ocean, make it difficult to explore these processes. Here, we set up an ultra-large volume, long-term incubation experiment to investigate how particulate organic matter impacts the shift of microbial population composition, and how nitrifiers impact the processing of organic matter.

2. Materials and methods

2.1. Experiment setup

The Aquatron facility (https://www.dal.ca/dept/aquatron.html), located at Dalhousie University, Canada, which is 10.64 m in depth and 3.66 m in diameter with an approximate volume of 117,000 L and has the ability of providing a large-volume, high-quality, temperature-controlled seawater and freshwater year round under professional management, was used to conduct the incubation experiment.

The long-term indoor incubation was set up to explore the impacts of autotrophic microbes on the energy and carbon-scarce ecosystem and reveal the microbial-driven mechanism(s) of biogeochemical cycling. Seawater was collected from the Halifax coast and filtered with 300-μm-pore-size bolting cloth before being used to fill the Aquatron tank. The incubation was performed under dark conditions for 73 days. Biogeochemical and molecular sampling were carried out at the tank surface (TS, depth ~ 1 m) and the tank bottom (TB, depth ~ 9 m). Detailed sampling schedules can be found in Table S1.

2.2. Biogeochemical analysis

Temperature and salinity were recorded by a Multiparameter Sonde (YSI EXO, YSI Incorporated, USA). Samples for nutrients were analyzed using a Skalar SAN^{++} autoanalyzer in Dalhousie University (Burt et al., 2013; Shi and Wallace, 2018). The concentration of dissolved oxygen (DO) and biological oxygen demand (BOD) were determined using the Winkler method (Carpenter, 1965; Grigoryeva et al., 2020). The five-day biological oxygen demand (BOD5) was measured based on the difference of BODs before and after a 5-day dark incubation. The chemical oxygen demand (COD_{Mn}) was measured using the alkaline potassium permanganate method based on specification GB 17378.4–2007 (Liu et al., 2018; Yang et al., 2019).

2.3. Particulate material analysis

For particulate material analysis, 1L to 4L of seawater was filtered through pre-combusted (450 °C for 4 h) 0.7-μm-pore-size glass microfiber filters (GF/F, 25 mm diameter, Whatman). Filters were then placed in sterile petri dishes (25 mm diameter, Whatman), which were previously washed by 1 mol L^{-1} hydrochloric acid and rinsed with Milli-Q water, and immediately stored at −20 °C until further analysis.

The filters with particulate material were freeze dried for 24 h using freeze dryer (FREEZONE 6, Labconco, USA) and then fumed with concentrated HCL vapor for 48 h. The filters were next washed with Milli-Q water until the pH was neutral and then dried at 60 °C to a constant weight. Finally, they were stored in sealed petri dishes until further analysis. Particulate organic carbon (POC) and particulate nitrogen (PN) were analyzed using a continuous-flow elemental analyzer (Flash EA 1112 HT) coupled to an isotope ratio mass spectrometer (Thermo Finnigan Delta V Advantage) system. Helium was used as the carrier gas at a flow rate of 90 mL min^{-1}. The temperature of the reaction column and chromatographic column were 960 °C and 50 °C, respectively.

The chemical composition of the particulate organic matter was analyzed using pyrolysis–gas chromatography-mass spectrometry (Çoban-Yıldız et al., 2006). Approximately 6 mg of particulate matter was placed into a quartz tube and moistened with 100 μL of tetramethylammonium hydroxide (25% in methanol) solution. The samples were pyrolyzed at 550 °C using a single point pyrolyzer (Frontier Laboratories Ltd., Japan) connected to a gas chromatograph-mass spectrometer (QP2010, Shimadzu, Japan). Helium was used as carrier gas and the flow rate was 1.8 mL min^{-1}. The column temperature was initially set at 40 °C for 3 min, then heated to 300 °C at a rate of 10 °C min^{-1} and maintained for 15 min. The mass spectrometer was operated at an ionization energy of 70 eV (EI). The mass detection range (m/z) was 25–500 and the cycle time was 1 s. Pyrolysis products were quantified by peak height, and the National Institute of Standards and Technology Mass Spectral Library database, published spectra, and real standards were used to identify the obtained mass spectra.

2.4. Molecular analyses

Three to five liters of seawater for molecular analyses were successively filtered through 3, 0.8, and 0.2-μm-pore-size polycarbonate filters (47 mm diameter; Millipore) at a pressure of <0.03 MPa. Then the filters were stored in RNase-free tubes with 1.5 mL RNA*later* RNA stabilization solution (Ambion) at −20 °C until RNA extraction. Soil RNA Mini Kit (R6825, Omega Bio-Tek, Norcross, GA, USA) was used to extract total RNA, according to manufacturer's protocols. Reverse transcription reactions were performed using the FastQuantity RT Kit (KR106) (Tiangen biochemical technology, Beijing, China) to generate cDNA. The bacterial V3–V4 regions of 16S rRNA genes were amplified using primers 341F (5′-CCTAYGGGRBGCASCAG-3′) and 806R (5′-GGACTACNNGGGTATCTAAT-3′) fused with a unique eight-base barcode for each sample (Zhang et al., 2016). PCR reactions were performed in triplicate 50 μL mixture containing 100 ng of template, 5 μL of 2.5 mM dNTPs, 5 μL of 10 × KOD Buffer, 1.5 μL of each primer (5 μM) and 1 μL of KOD Polymerase, and 100 ng of template cDNA. Thermal cycle consisted of an initial denaturation at 95 °C for 2 min, 27 cycles at 98 °C for 10 s, 62 °C for 30 s, and 68 °C for 30 s and a final extension at 68 °C for 10 min. Amplicons were purified using the AxyPrep DNA Gel Extraction Kit (Axygen Biosciences, Union City, CA, U.S.) and pooled in equimolar concentrations for paired-end sequencing (2 × 250 bp) on an Illumina platform according to the standard protocols.

Low quality raw reads, containing less than 60% bases (Q-value > 20), or those with greater than 10% ambiguous bases (N) were eliminated. Then, FLASH (Magoc and Salzberg, 2011) software was used to merge paired-end clean reads with a minimum overlap of 10 bp and mismatch error rates of 2%. Next, QIIME v1.9.1 (Caporaso et al., 2010) was used to denoise merged reads under specific filtering conditions based on Bokulich et al. (2013). Clean sequences were aligned to the reference database (http://drive5.com/uchime/uchime_download.html), and chimera checking was performed by UCHIME algorithm (http://www.drive5.com/usearch/manual/uchime_algo.html). Clean, non-chimeric sequences were clustered into operational taxonomic units (OTUs) of >97% similarity using UPARSE pipeline (Edgar, 2013). To assign taxonomy, representative sequences with highest abundance in each OTU cluster was checked against the SILVA database (Pruesse et al., 2007) using RDP classifier (Wang et al., 2007) with confidence threshold values ranged from 0.8 to 1. FAPROTAX (Louca et al., 2016; Li et al., 2019) was used for predicting ecological functions.

2.5. Statistical analyses

Statistical analyses were carried out using the vegan package (Oksanen, 2011) in R unless otherwise stated. Alpha diversity estimations (Chao1, Shannon, and Good's coverage) based on OTUs assignment were calculated in QIIME. To display and compare the compositions of pyrolysis-derived compounds of particulate organic matter (POM) among different samples, principal component analysis (PCA; Abdi and Williams, 2010) was performed using the Z-transformed

contents (area%) of particulate pyrolysis-derived compounds and visualized by packages ggbiplot in R. Nonmetric multidimensional scaling (NMDS) analysis was conducted in R to determine the similarity of samples, using a distance matrix constructed from Bray-Curtis dissimilarity of bacterial community composition (phylum level) and predicted functional profiles based on FAPROTAX. The variations in bacterial communities under the constraint of environment parameters was analyzed by redundancy analysis (RDA), the relative abundance and environment parameters were Z-normalized and multicollinear environment variables as indicated by variance inflation factors (VIF > 10) were eliminated from subsequent analyses. The statistical significance of the fractions of variance was tested using Monte Carlo permutation tests (999 permutations) and only significant explanatory parameters ($p < 0.05$) were displayed in the plot. The correlations between community compositions of nitrifiers (OTU level) from different size fractions and different explanatory parameters were examined by Mantel test, dissimilarity matrices of communities of nitrifiers were depended on Bray-Curtis distances between samples. Kendall and Spearman tests were run to determine the correlations between the contents (area%) of particulate nitrogenous compounds and the relative abundances of *Nitrospinae* for the samples from 0.8 - 3 μm and >3 μm size fractions.

For network analyses, Spearman's rank correlations between OTUs and the contents (area%) of different particulate pyrolysis-derived compounds were calculated in R for the samples from different size fractions, respectively. Only correlations with $-0.8 < r < 0.8$ and $p < 0.05$ were retained as valid co-occurrence events, networks were visualized using the interactive platform gephi (Bastian et al., 2009) with Fruchterman-Reingold force-directed layout algorithm.

3. Results

3.1. Changes in POM characteristics and other biogeochemical parameters

The changes in physical–chemical parameters showed similar trends between TS and TB. The salinity was constant, indicating that the system was stable (Fig. S1A). In both TS and TB, the temperature increased and then decreased over the incubation period (Fig. S1B). While the temperature was higher in TS than that in TB during the first 48 days, the temperature showed no obvious difference between TS and TB for the remainder of the incubation (Fig. S1B). The concentration of DO showed a decreasing trend, but the environment in the Aquatron was always oxic (Fig. 1A). The concentration of ammonium decreased from 3.31 and 3.36 to 0 μM in TS and TB, respectively, over the course of the first 40 days, and then increased from 0 to 0.2 μM by day 73 in TS and 0.36 μM on day 56 in TB (Fig. 1D). The concentration of nitrite was ≤ 0.8 μM throughout the incubation in both TS and TB. The concentration of nitrate increased in TS, peaking on day 40 (10.40 μM), followed by a slight decrease. In TB, the concentration of nitrate decreased before day 12, after which it increased again, reaching a peak on day 56 (10.56 μM) (Fig. 1D). Overall, during the 73 d incubation, ammonium was oxidized to nitrate and the total concentration of DIN increased slightly (Fig. 1D). The concentrations of silicate and phosphate increased slightly in TS, but dramatically decreased in TB from day 0 to day12 and then increased from day 12 to day 24, followed by a weak increasing trend for the remainder of the incubation (Fig. 1B and C).

The POC concentration decreased from 27.6 to 16.9 μg L^{-1} in TS and from 33.2 to 19.3 μg L^{-1} in TB. The POC:PN ratio also displayed a decreasing trend from 6.8 to 4.0 in TS and from 6.6 to 3.6 in TB (Fig. 2A). Over the course of the incubation, there was a general, relative increase in the abundances of nitrogenous compounds and aromatic compounds within the particulate chemical compositions (Fig. 2B). Principal component analysis (PCA) of POM chemical composition showed that the first two dimensions explained 56% and 75.4% of the total variance in the POM composition in TS and TB, respectively (Fig. 2C and D). Samples were divided into two different clusters in the PCA biplot. The samples collected after day 24 in TS (Fig. 2C) and day 32 in TB (Fig. 2D) were characterized by compounds containing greater amounts of nitrogen, ring structures (benzene or non-benzene), and alkane. However, before day 24 in TS and day 32 in TB, the samples were characterized by

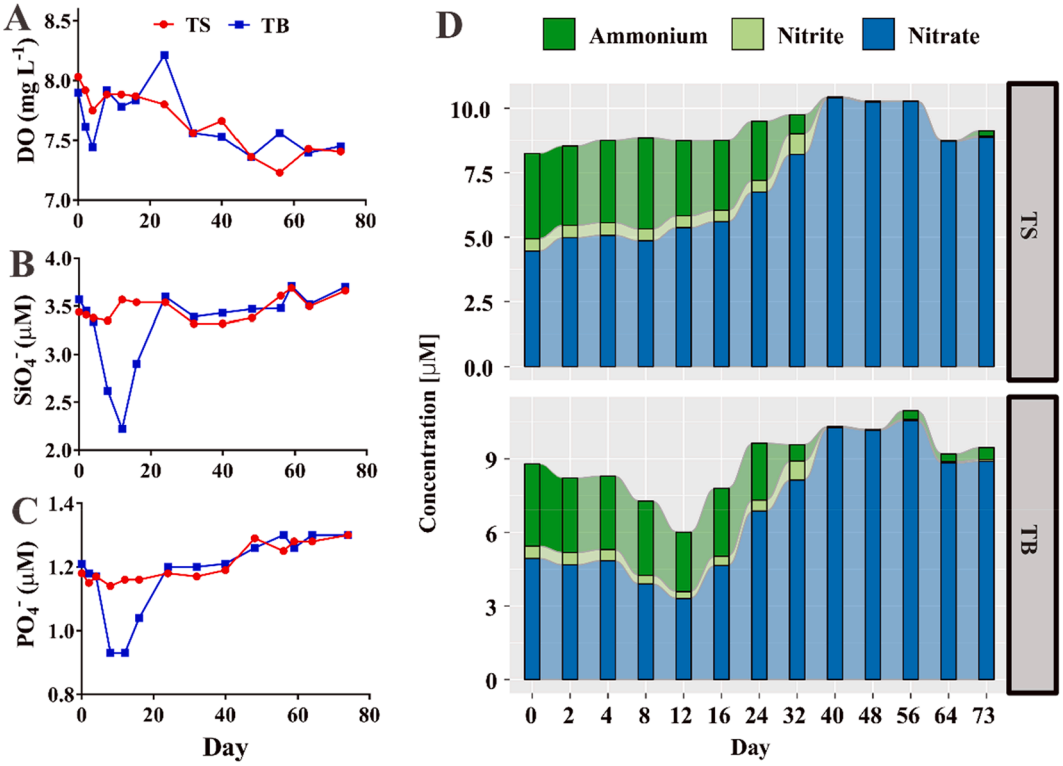

Fig. 1. Changes in (A) dissolved oxygen (DO), (B) silicate, (C) phosphate, and (D) dissolved inorganic nitrogen (DIN). TS, tank surface; TB, tank bottom.

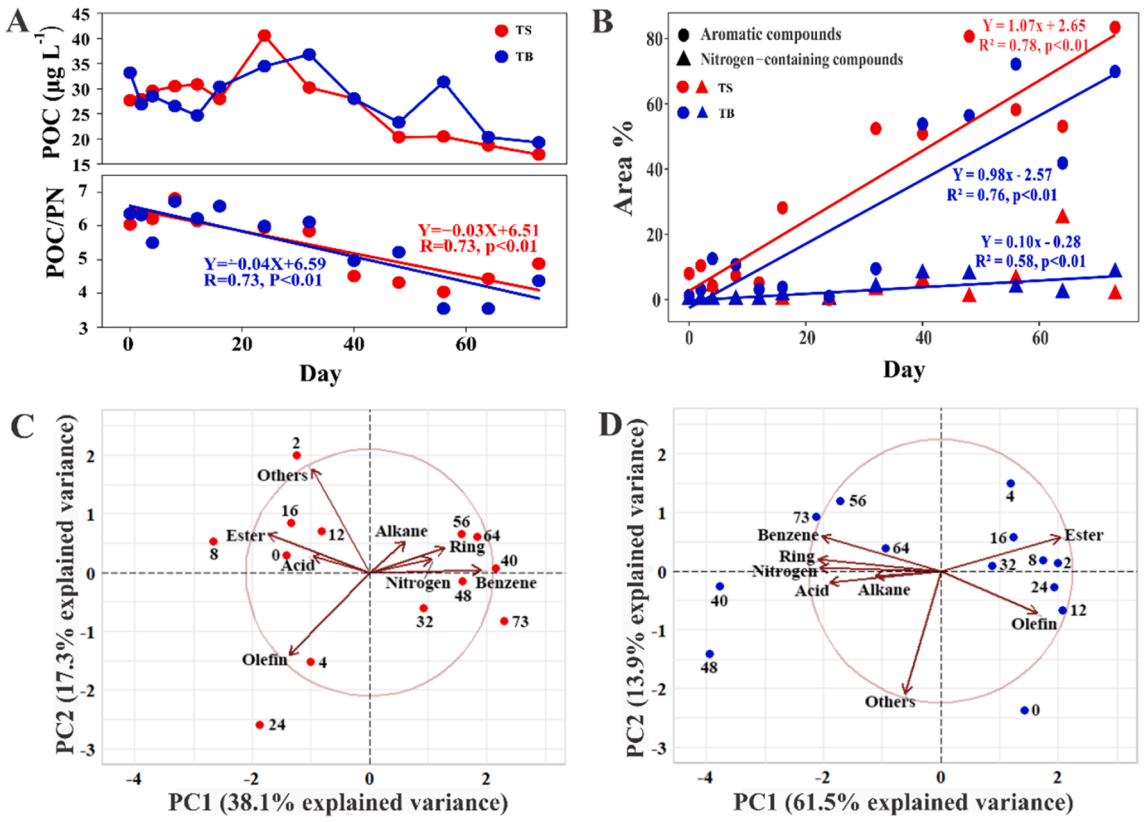

Fig. 2. (A) Concentration of particulate organic carbon (POC) and ratio of POC to particulate nitrogen (POC:PN). (B) Changes in relative abundance of aromatic and nitrogen-containing compounds. Principal component (PC1 × PC2) plots generated from particulate organic matter compositions in (C) the tank surface (TS) and (D) bottom (TB). Numbers represent sampling time (day). Axes percentages represent the proportion of variance explained by each principal component. Arrows represent variables and circles are correlation circles that the closer variables are to, the more important they are to interpret the principal components.

greater amounts of ester and olefin. Besides, the change of acid with time in the samples had an opposite trend between TS and TB. There was more acid before day 24 in TS and after day 32 in TB (Fig. 2C and D).

3.2. Bacterial community composition

The bacterial community structure was analyzed at three cell-size fractions. The bacterial diversity and species richness of all three size fractions increased with incubation time (Fig. S2). The bacterial

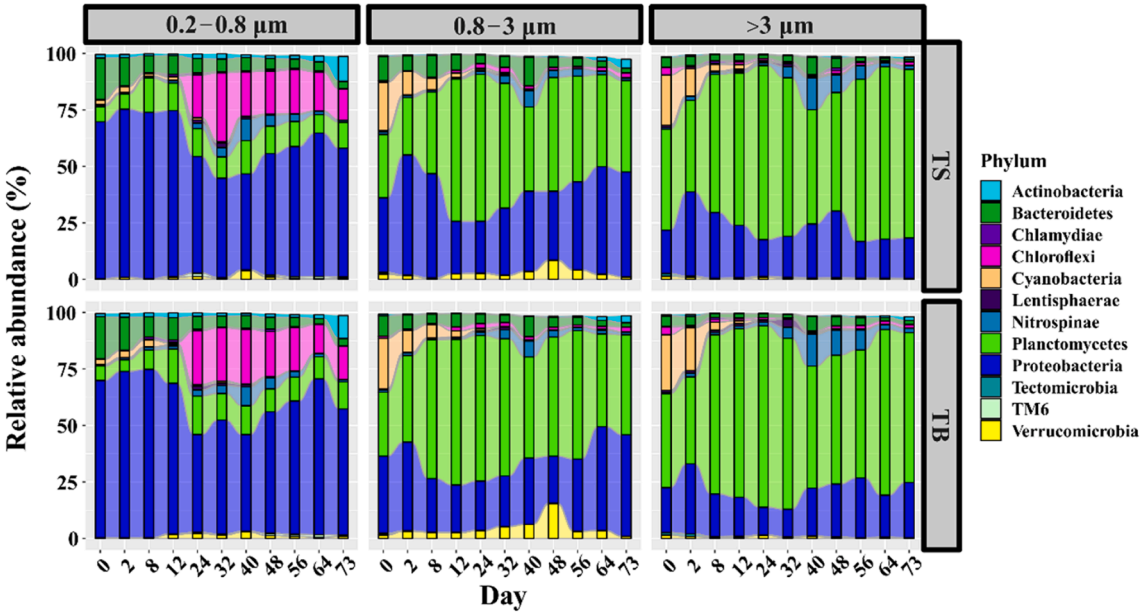

Fig. 3. Bacterial community composition at the phylum level based on 16S rRNA gene libraries in the 0.2–0.8 μm, 0.8–3 μm, and > 3 μm size fractions. TS, tank surface; TB, tank bottom.

communities of the 0.8–3 μm cell-size fraction were more similar to those of the >3 μm fraction than the 0.2–0.8 μm fraction (Fig. S3A and B). *Bacteroidetes*, *Cyanobacteria, Chloroflexi, Nitrospinae, Proteobacteria*, and *Planctomycetes* were the dominant phyla in the Aquatron tower (Fig. 3). Among these phyla, OTUs assigned to *Cyanobacteria*, *Nitrospinae*, and *Planctomycetes* were more abundant in the 0.8–3 μm and >3 μm cell-size fractions than that in the 0.2–0.8 μm fraction while the opposite pattern was observed for OTUs affiliated with *Bacteroidetes*, *Chloroflexi*, and *Proteobacteria* (Fig. 3).

As incubation time increased, there was a striking shift of phylogenetic groups in all size fractions (Fig. 3). The relative abundance of *Cyanobacteria*, which dominated the > 0.8 μm communities at the beginning of the incubation, decreased over time and had almost disappeared after day 24. In contrast, the relative abundance of *Nitrospinae* increased starting at day 12 and then decreased after day 40 (Fig. 3). In the 0.2–0.8 μm communities, the relative abundance of *Bacteroidetes* decreased with time, while *Chloroflexi* increased sharply after day 12 and then remained constant (Fig. 3). In contrast to the above groups, the relative abundances of *Planctomycetes* and *Proteobacteria* remained relatively constant and were prominent phyla throughout the incubation.

3.3. Potential microbial metabolism in the Aquatron system

Functional profiles of the bacterial communities were predicted based on population composition using FAPROTAX. The results indicated that metabolism within the system was dominated by aerobic chemoheterotrophy and nitrification (Fig. 4). Sequences assigned to chemoheterotrophy and aerobic chemoheterotrophy were consistently significantly higher than other groups during the incubation. Sequences related to light-dependent reactions (phototrophy, photoautotrophy, chloroplasts) were enriched in the 0.8–3 and >3 μm fractions, but their relative abundance decreased over the course of the incubation, while the contribution of sequences involved in nitrification increased and peaked on day 40 (Fig. 4). In addition, the relative abundances of sequences regulating the oxidation of sulfur compounds increased starting day 24 and peaked on day 56. Sequences associated with nitrogen fixation also increased after day 24 and was consistent with the trend in nitrification (Fig. 4).

Two-dimensional NMDS ordination was used to depict the similarities among functional profiles of the bacterial communities. While the bacterial communities were clearly separated into three clusters according to size fraction ($p < 0.01$; Fig. S3A and B), the functional profiles from the three size fractions displayed a large amount of overlap ($p < 0.01$) and the differences among the three clusters decreased with incubation time (Fig. S3C and D).

3.4. Relationships between microbial community and biogeochemical parameters

Network analysis of the relationship between OTUs and particle components indicated that metabolism related to nitrogen played an essential role in the incubation system, especially in the 0.8–3 and >3 μm bacterial communities (Fig. 5). Moreover, there were a greater number of positive correlations than negative correlations between OTUs and nitrogenous compounds in the 0.2–0.8 μm and >3 μm fractions, while the opposite pattern was observed in the 0.8–3 μm fraction (Fig. 5D). Besides nitrogen-related metabolism, processes related to ester and benzene metabolisms were also dominant. Notably, ester metabolisms were especially dominant in the 0.2–0.8 μm fraction, and benzene metabolisms were dominant especially in the >3 μm fraction (Fig. 5).

RDA analysis was further conducted to assess the relationships between bacterial communities and environmental variables (Fig. 6). Only the statistically significant biogeochemical parameters are shown in the RDA plot. The results indicated that ammonium was the only significant variable explaining the pattern of the bacterial community structures in TS ($p < 0.05$; Fig. 6A), while in TB the concentrations of ammonium and

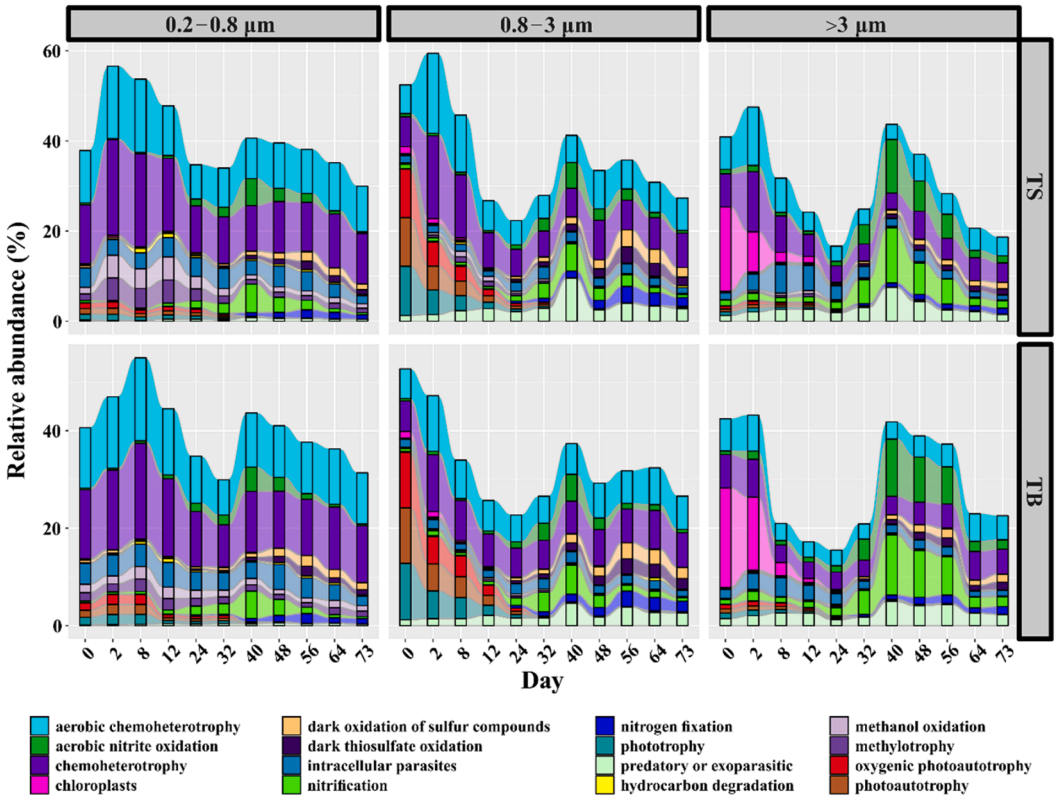

Fig. 4. Changes in functional metabolism (relative abundance ≥ 1%) predicted by FAPROTAX based on 16S rRNA gene libraries. TS, tank surface; TB, tank bottom.

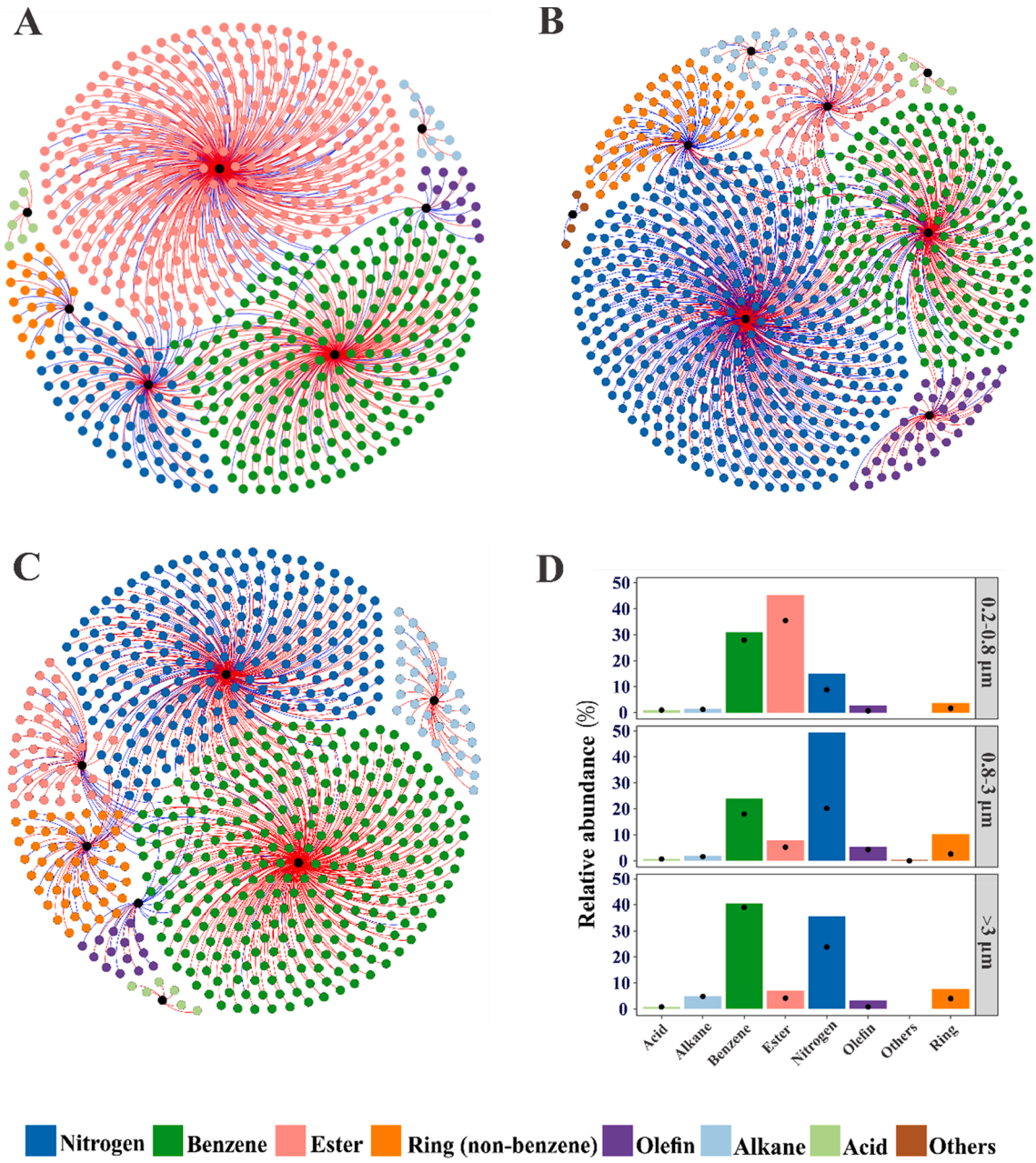

Fig. 5. Network interactions between OTUs in the (A) 0.2–0.8 μm, (B) 0.8–3 μm, and (C) > 3 μm size communities and particulate pyrolysis-derived compounds. Red and blue lines indicate positive and negative interactions between OTUs and particle components, respectively. Dark nodes represent particulate compounds. Colorful nodes represent OTUs, and the different colors represent different modules, which were divided based on different particulate compounds. Nodes involved in the modules have the highest correlations with the corresponding compounds. (D) The bar graph shows the relative abundance of colored nodes involved in each module in total nodes. The dark dots in the bars indicate the proportions of nodes that had positive correlations with particulate compounds in total nodes. (For interpretation of the references to color in this figure legend, the reader is referred to the web version of this article.)

nitrite were the significant explanatory variables for the shift of bacterial community structure (Fig. 6).

Since ammonium and nitrite were the most important factors shaping the bacterial communities in this system, nitrification could be the essential process. Further correlations between nitrifiers such as *Nitrospinae* and *Nitrospirae* and biogeochemical parameters were analyzed using the Mantel test (Fig. 7). The results showed that the concentrations of ammonium and nitrate were positively associated with the community structure of nitrifiers in all size fractions of both TS and TB, with the exception of the 0.8–3 μm fraction in TB. POC:PN was positively associated with the community structure of nitrifiers in all size fractions of both TS and TB, except for the 0.2–0.8 μm and 0.8–3 μm fractions in TB. Temperature was also an important factor, positively correlating with the community structure of nitrifiers in all size fractions of both TS and TB, except for the >3 μm fraction in TS. In addition, the concentrations of nitrite and DO were positively associated with the community structure of nitrifiers in the >3 μm fraction (Fig. 7). Notably, DO had more positive correlations with other biogeochemical parameters in TB than in TS, albeit it showed no strong correlation with nitrifiers (Fig. 7).

The correlations between the relative abundances of nitrifiers and POM chemical compositions were also analyzed (Table S2). The results indicated that the relative abundance of *Nitrospinae*, within the 0.8–3 and >3 μm size fractions was positively related to the relative abundance of particulate compounds containing nitrogen. In TS, *Nitrospinae* from the 0.8–3 μm size fraction had a stronger positive correlation with

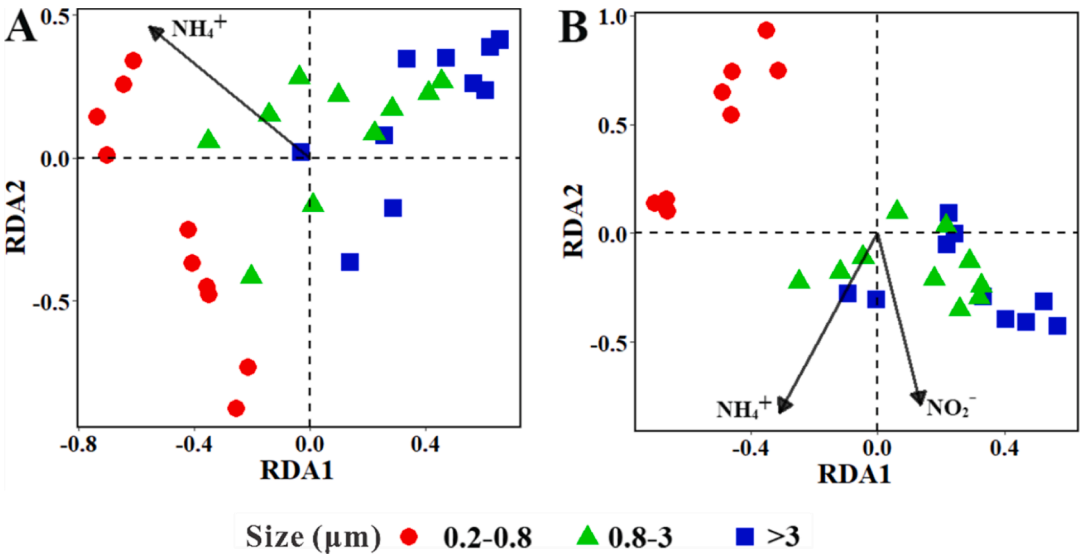

Fig. 6. Redundancy analysis of the 0.2–0.8 μm, 0.8–3 μm, and > 3 μm size bacterial communities under biogeochemical constraints in (A) the tank surface and (B) bottom. Each square, point, or triangle represents an individual community. Vectors represent biogeochemical variables (Monte Carlo permutation test: $p < 0.05$). NO_2^-, nitrite; NH_4^+, ammonium.

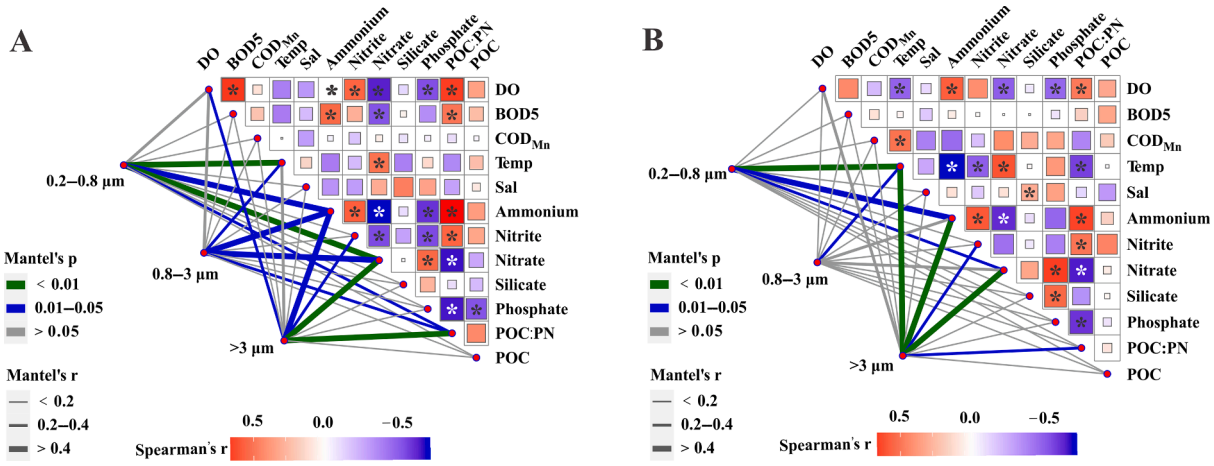

Fig. 7. Correlations between nitrifier community compositions (based on OTUs) and biogeochemical parameters as well as correlations between biogeochemical parameters in (A) the tank surface and (B) bottom. The width of grey lines indicates the r-value of the Mantel test; the color of lines indicates the *p*-value. Asterisks indicate Spearman's $p < 0.05$ and the color bar is based on Spearman's correlation coefficients. DO, dissolved oxygen; BOD5, biological oxygen demand; COD_{Mn}, chemical oxygen demand; Temp, temperature; Sal, salinity; POC, particulate organic carbon (concentration); PN, particulate nitrogen.

nitrogenous compounds than those from the >3 μm fraction, while a stronger correlation was observed in the >3 μm size fraction of TB (Table S2).

4. Discussion

It was observed that phototrophic groups decreased while chemoautotrophic nitrifiers increased over the course of time in the Aquatron incubation system. Ammonium, as a substrate of nitrification, was found to be significantly correlated with nitrifiers, and thus is an important parameter explaining the shift in total bacterial community compositions in the Aquatron system. The degradation of organic matter could release ammonium into the surrounding environment and then influence the nitrifiers' activities (Bartl et al., 2019; Wu et al., 2001). When labile organic matter derived from photoautotrophs was depleted, degradation of organic compounds produced from chemoautotrophic nitrifiers and the promoted degradation of recalcitrant compounds could release new ammonium into the environment, as indicated by the slight accumulation of ammonium after over 40 days of incubation (Fig. 1D). The accumulation of nitrate, accompanied by the increase of the relative abundance of the nitrifiers, indicated that the nitrification was occurring in the Aquatron tower, driving the biogeochemical and energy cycles. Function prediction also supported that chemoautotrophy, especially nitrification, was an essential process. Notably, while there were distinct differences in the bacterial community compositions among the three size fractions, their functional profiles were relatively consistent at the late stage of the experiment, primarily consisting of chemoheterotrophy, nitrification, and other metabolisms related to nitrogen.

Previous research suggested that temperature was an important parameter controlling organic matter degradation (Cheng et al., 2017), and thus temperature could also show a correlation with nitrifiers (Fig. 7). As indicated by the RDA analysis, ammonium was a more important parameter determining microbial communities in this system after colinear variables (e.g. temperature, etc.) were removed (Fig. 6). Previous research also suggested that temperature had minor effects on nitrifier communities when other environmental parameters changed

dramatically (Barnard et al., 2005; Séneca et al., 2020). This hinted to us that many parameters including temperature could impact nitrifiers, yet substrates were the most important ones. In addition, previous research suggested that while organic compounds are resistant to microbial degradation at the surface, they can be served as substrates at greater depths with higher pressure (Boutrif et al., 2011). Thus, although the impact of pressure on the microbial community could be slight in the Aquatron tank with a depth of 10 m, hydrostatic pressure could influence the microbial metabolism of organic and inorganic substrates in the real deep ocean (Tamburini et al., 2013).

With the degradation of organic matter and the relative increase in abundance of particle-associated nitrifier *Nitrospinae*, the chemical composition of the particles changed, resulting in the relative abundances of particulate nitrogenous compounds increasing over the course of the incubation. The decrease of the POC:PN ratio also supports the finding that the proportion of nitrogenous compounds increased with incubation time. Furthermore, positive correlations were observed between the particle-associated *Nitrospinae* and particulate nitrogenous compounds, suggesting that nitrifiers contributed the increase of relative abundance of nitrogenous compounds. We speculated that the nitrifiers could produce a suite of organic compounds that resulted in the altered organic matter composition. Recent research has suggested that the organic compounds excreted by AOA are dominated by nitrogenous compounds (Bayer et al., 2019).

Nitrifier recruitment from the incubation system and the increased proportion of compounds containing nitrogen could drive shifts within the active microorganism community structure and function in the starved dark ecosystem (Sebastián et al., 2018). Fresh organic carbon excreted by these nitrifying microorganisms could further trigger a 'priming effect' that promotes the degradation of relatively unreactive organic matter (Kuzyakov et al., 2000).

In our incubation system, particulate organic matter composition showed that compounds containing ring structures (mainly benzene ring) were important components in POM especially in the later stage of the incubation. It is well known that aromatic compounds are recalcitrant to bacterial degradation in general (Hansen et al., 2016; O'Donnell et al., 2016) and accumulate not only in many incubation experiments (Jiao et al., 2018; Zheng et al., 2019) but also in the deep ocean (Medeiros et al., 2015). Our microbial analysis found that in the Aquatron system, *Chloroflexi* became an abundant group after day 12. Genomic evidence supports that *Chloroflexi* play important roles in the degradation of aromatic compounds (Wasmund et al., 2014; Landry et al., 2017; Colatriano et al., 2018). Some groups affiliated with the *Planctomycetes* and *Proteobacteria* are also able to degraded aromatic compounds (Hilyard et al., 2008; Zhang et al., 2019). Moreover, network analysis showed that metabolisms related to aromatic compound (e.g. benzene) degradation were important in this study system. A previous study also indicated that a microbial community evolves to be more correlated with less labile compounds, such as aromatic compounds, during the later stage of incubation (Wu et al., et al., 2018). Our results also reflected this evolution. At the early stage of incubation, POM chemical compositions were characterized by greater amounts of ester, as indicated by the PCA analysis (Fig. 2C and D). Esters were served as important energy storage components (Ishige et al., 2003; Wältermann and Steinbüchel, 2005), and therefore tight correlations between bacterial OTUs and esters were observed by the network analysis in this dark system (Fig. 5). With the degradation of esters, POM was characterized by compounds containing greater amounts of nitrogen and ring structures (benzene or non-benzene), and these compounds metabolisms were the dominant process in the network interactions. It has been reported that degradation of labile or semi-labile organic matter can help microorganisms overcoming the resonance energy that stabilizes the aromatic ring, which is the crucial step in the degradation of aromatic compounds (Fuchs et al., 2011). Coupling the enrichment of nitrifiers, enhancement of nitrification with degradation of nitrogenous compounds and aromatic compounds in the incubation, we speculate that fresh organic carbon produced by the nitrifiers could promote the degradation of recalcitrant aromatic compounds.

Through an ultra-large volume, long-term incubation this study investigated the relationships between particulate organic matter and microbial population composition and how nitrifiers impact organic matter processing. The results indicated that nitrifiers were enriched and nitrification are strengthened in the starved aphotic ecosystem. Organic matter degradation could provide an ammonium source for the enhancement of nitrification. The nitrogenous compounds of particulate materials became more important, with the ratio of carbon to nitrogen decreasing over the course of the incubation. This could be attributed to the organic compounds produced by the nitrifiers. Furthermore, the microbial metabolisms related to nitrogenous and aromatic compounds were enhanced. This study highlights potential contribution of nitrifiers to organic matter processing in the starved dark ecosystem.

Credit authorship statement

Lianbao Zhang: Data curation, Formal analysis, Visualization, Investigation, Writing-original draft. **Mingming Chen:** Writing - review & editing. **Xiaowei Chen:** Investigation. **Jianning Wang:** Investigation. **Yu Zhang:** Investigation. **Xilin Xiao:** Investigation. **Chen Hu:** Investigation. **Jihua Liu:** Project administration. **Rui Zhang:** Supervision. **Dapeng Xu:** Supervision. **Nianzhi Jiao:** Funding acquisition, Project administration, Supervision. **Yao Zhang:** Conceptualization, Funding acquisition, Project administration, Supervision, Writing - review & editing.

Declaration of Competing Interest

The authors declare that they have no known competing financial interests or personal relationships that could have appeared to influence the work reported in this paper.

Acknowledgments

We sincerely thank all members of Aquatron team for their assistance in the experiment, especially Prof. Douglas Wallace, Prof. Julie Laroche, Prof. Hugh Macintyre, and Dr. Qiang Shi for their assistance in data analyses, Elizabeth Kerrigan for her assistance in the nutrient measurements, John Batt and Claire Normandeau for their technical assistance in using the laboratory's equipments, and Steve Fowler for his assistance in the sample transportation. We also thank Jia Sun and Jiezhen Xie for their help in sampling. This work was funded by the National Key Research and Development Program (2016YFA0601400), NSFC projects (92051114, 91751207, U1805242, 41721005, and 41861144018), and Fundamental Research Funds for the Central Universities (20720200070). This study is a contribution to the international IMBeR project.

Appendix A. Supplementary material

Supplementary data to this article can be found online at https://doi.org/10.1016/j.envint.2021.106776.

References

Abdi, H., Williams, L.J., 2010. Principal component analysis. Wiley Interdiscip. Rev. Comput. Stat. 2, 433–459.

Arístegui, J., Duarte, C.M., Agustí, S., Doval, M.D., Álvarez-Salgado, X.A., Hansell, D.A., 2002. Dissolved organic carbon support of respiration in the dark ocean. Science 298, 1967–1967.

Arístegui, J., Gasol, J.M., Duarte, C.M., Herndld, G.J., 2009. Microbial oceanography of the dark ocean's pelagic realm. Limnol. Oceanogr. 54 (5), 1501–1529.

Arístegui, J., Montero, M.F., 2005. Temporal and spatial changes in plankton respiration and biomass in the Canary Islands region: the effect of mesoscale variability. J. Mar. Syst. 54 (1-4), 65–82.

Baltar, F., Arístegui, J., Gasol, J.M., Sintes, E., Herndl, G.J., 2009. Evidence of prokaryotic metabolism on suspended particulate organic matter in the dark waters of the subtropical North Atlantic. Limnol. Oceanogr. 54 (1), 182–193.
Bartl, I., Hellemann, D., Rabouille, C., Schulz, K., Tallberg, P., Hietanen, S., Voss, M., 2019. Particulate organic matter controls benthic microbial N retention and N removal in contrasting estuaries of the Baltic Sea. Biogeosciences 16 (18), 3543–3564.
Barnard, R., Leadley, P.W., Hungate, B.A., 2005. Global change, nitrification, and denitrification: a review. Global Biogeochem. Cycles 19 (1). https://doi.org/10.1029/2004GB002282.
Bastian, M., Heymann, S., Jacomy, M., 2009. Gephi: an open source software for exploring and manipulating networks. In: Proceedings of the International AAAI Conference on Web and Social Media, vol. 3(1).
Bayer, B., Hansman, R.L., Bittner, M.J., Noriega-Ortega, B.E., Niggemann, J., Dittmar, T., Herndl, G.J., 2019. Ammonia-oxidizing archaea release a suite of organic compounds potentially fueling prokaryotic heterotrophy in the ocean. Environ. Microbiol. 21, 4062–4075.
Bokulich, N.A., Subramanian, S., Faith, J.J., Gevers, D., Gordon, J.I., Knight, R., Mills, D. A., Caporaso, J.G., 2013. Quality-filtering vastly improves diversity estimates from Illumina amplicon sequencing. Nat. Methods 10, 57.
Boutrif, M., Garel, M., Cottrell, M.T., Tamburini, C., 2011. Assimilation of marine extracellular polymeric substances by deep-sea prokaryotes in the NW Mediterranean Sea. Environmental microbiology reports 3, 705–709.
Buesseler, K.O., Lamborg, C.H., Boyd, P.W., Lam, P.J., Trull, T.W., Bidigare, R.R., Bishop, J.K.B., Casciotti, K.L., Dehairs, F., Elskens, M., Honda, M., Karl, D.M., Siegel, D.A., Silver, M.W., Steinberg, D.K., Valdes, J., Van Mooy, B., Wilson, S., 2007. Revisiting carbon flux through the ocean's twilight zone. Science 316 (5824), 567–570.
Burt, W.J., Thomas, H., Fennel, K., Horne, E., 2013. Sediment-water column fluxes of carbon, oxygen and nutrients in Bedford Basin, Nova Scotia, inferred from 224 Ra measurements. Biogeosciences 10, 53–66.
Caporaso, J.G., Kuczynski, J., Stombaugh, J., Bittinger, K., Bushman, F.D., Costello, E.K., Fierer, N., Peña, A.G., Goodrich, J.K., Gordon, J.I., Huttley, G.A., Kelley, S.T., Knights, D., Koenig, J.E., Ley, R.E., Lozupone, C.A., McDonald, D., Muegge, B.D., Pirrung, M., Reeder, J., Sevinsky, J.R., Turnbaugh, P.J., Walters, W.A., Widmann, J., Yatsunenko, T., Zaneveld, J., Knight, R., 2010. QIIME allows analysis of high-throughput community sequencing data. Nat. Methods 7 (5), 335–336.
CARPENTER, J.H., 1965. The Chesapeake Bay Institute technique for the Winkler dissolved oxygen method. Limnol. Oceanogr. 10 (1), 141–143.
Cheng, L., Zhang, N., Yuan, M., Xiao, J., Qin, Y., Deng, Y., Tu, Q., Xue, K., Nostrand, J.D. V., Wu, L., He, Z., Zhou, X., Leigh, M.B., Konstantinidis, K.T., Schuur, E.A., Luo, Y., Tiedje, J.M., Zhou, J., 2017. Warming enhances old organic carbon decomposition through altering functional microbial communities. ISME 11, 1825–1835.
Çoban-Yıldız, Y., Fabbri, D., Baravelli, V., Vassura, I., Yılmaz, A., Tuğrul, S., Eker-Develi, E., 2006. Analytical pyrolysis of suspended particulate organic matter from the Black Sea water column. Deep Sea Res. Part II 53 (17-19), 1856–1874.
Colatriano, D., Tran, P.Q., Guéguen, C., Williams, W.J., Lovejoy, C., Walsh, D.A., 2018. Genomic evidence for the degradation of terrestrial organic matter by pelagic Arctic Ocean Chloroflexi bacteria. Communications biology 1, 90.
Edgar, R.C., 2013. UPARSE: highly accurate OTU sequences from microbial amplicon reads. Nat. Methods 10, 996.
Fuchs, G., Boll, M., Heider, J., 2011. Microbial degradation of aromatic compounds—from one strategy to four. Nat. Rev. Microbiol. 9 (11), 803–816.
Grigoryeva, N.I., Zhuravel, E.V., Mazur, A.A., 2020. Seasonal Variations of Water Quality in the Vostok Bay, Peter the Great Gulf, the Sea of Japan. Water Resour. 47 (2), 249–256.
Hansen, A.M., Kraus, T.E.C., Pellerin, B.A., Fleck, J.A., Downing, B.D., Bergamaschi, B.A., 2016. Optical properties of dissolved organic matter (DOM): Effects of biological and photolytic degradation. Limnol. Oceanogr. 61 (3), 1015–1032.
Hilyard, E.J., Jones-Meehan, J.M., Spargo, B.J., Hill, R.T., 2008. Enrichment, isolation, and phylogenetic identification of polycyclic aromatic hydrocarbon-degrading bacteria from Elizabeth River sediments. Appl. Environ. Microbiol. 74 (4), 1176–1182.
Ishige, T., Tani, A., Sakai, Y., Kato, N., 2003. Wax ester production by bacteria. Curr. Opin. Microbiol. 6 (3), 244–250.
Jiao, N., Cai, R., Zheng, Q., Tang, K., Liu, J., Jiao, F., Wallace, D., Chen, F., Li, C., Amann, R., Benner, R., Azam, F., 2018. Unveiling the enigma of refractory carbon in the ocean. Nat. Sci. Rev. 5 (4), 459–463.
Karner, M.B., DeLong, E.F., Karl, D.M., 2001. Archaeal dominance in the mesopelagic zone of the Pacific Ocean. Nature 409, 507.
Kuzyakov, Y., Friedel, J.K., Stahr, K., 2000. Review of mechanisms and quantification of priming effects. Soil Biol. Biochem. 32 (11-12), 1485–1498.
Landry, Z., Swan, B.K., Herndl, G.J., Stepanauskas, R., Giovannoni, S.J., 2017. SAR202 genomes from the dark ocean predict pathways for the oxidation of recalcitrant dissolved organic matter. MBio 8, e00413–e417.
Li, A.-Z., Han, X.-B., Zhang, M.-X., Zhou, Y., Chen, M., Yao, Q., Zhu, H.-H., 2019. Culture-Dependent and -Independent Analyses Reveal the Diversity, Structure, and Assembly Mechanism of Benthic Bacterial Community in the Ross Sea. Antarctica. Frontiers in microbiology 10. https://doi.org/10.3389/fmicb.2019.0252310.3389/fmicb.2019.02523.s001.
Liu, Z., Qiuqian, L., Yao, Z., Wang, X., Huang, L., Zheng, J., Wang, K., Li, L., Zhang, D., 2018. Effects of a Commercial Microbial Agent on the Bacterial Communities in Shrimp Culture System. Front. Microbiol. 9, 2430.
Louca, S., Parfrey, L.W., Doebeli, M., 2016. Decoupling function and taxonomy in the global ocean microbiome. Science 353 (6305), 1272–1277.
Magoc, T., Salzberg, S.L., 2011. FLASH: fast length adjustment of short reads to improve genome assemblies. Bioinformatics 27 (21), 2957–2963.
Medeiros, P.M., Seidel, M., Powers, L.C., Dittmar, T., Hansell, D.A., Miller, W.L., 2015. Dissolved organic matter composition and photochemical transformations in the northern North Pacific Ocean. Geophys. Res. Lett. 42 (3), 863–870.
O'Donnell, J.A., Aiken, G.R., Butler, K.D., Guillemette, F., Podgorski, D.C., Spencer, R.G. M., 2016. DOM composition and transformation in boreal forest soils: The effects of temperature and organic-horizon decomposition state. J. Geophys. Res. Biogeosci. 121 (10), 2727–2744.
Oksanen, J., 2011. Multivariate analysis of ecological communities in R: vegan tutorial [J]. R package version 1 (7), 1–43.
Pachiadaki, M.G., Sintes, E., Bergauer, K., Brown, J.M., Record, N.R., Swan, B.K., Mathyer, M.E., Hallam, S.J., Lopez-Garcia, P., Takaki, Y., Nunoura, T., Woyke, T., Herndl, G.J., Stepanauskas, R., 2017. Major role of nitrite-oxidizing bacteria in dark ocean carbon fixation. Science 358 (6366), 1046–1051.
Pruesse, E., Quast, C., Knittel, K., Fuchs, B.M., Ludwig, W., Peplies, J., Glockner, F.O., 2007. SILVA: a comprehensive online resource for quality checked and aligned ribosomal RNA sequence data compatible with ARB. Nucleic Acids Res. 35 (21), 7188–7196.
Raven, J.A., 2009. Contributions of anoxygenic and oxygenic phototrophy and chemolithotrophy to carbon and oxygen fluxes in aquatic environments. Aquat. Microb. Ecol. 56, 177–192.
Reinthaler, T., van Aken, H., Veth, C., Arístegui, J., Robinson, C., Williams, P.J.l.B., Lebaron, P., Herndl, G.J., 2006. Prokaryotic respiration and production in the meso- and bathypelagic realm of the eastern and western North Atlantic basin. Limnol. Oceanogr. 51 (3), 1262–1273.
Reinthaler, T., van Aken, H.M., Herndl, G.J., 2010. Major contribution of autotrophy to microbial carbon cycling in the deep North Atlantic's interior. Deep Sea Res. Part II 57 (16), 1572–1580.
Sebastián, M., Auguet, J.-C., Restrepo-Ortiz, C.X., Sala, M.M., Marrasé, C., Gasol, J.M., 2018. Deep ocean prokaryotic communities are remarkably malleable when facing long-term starvation. Environ. Microbiol. 20 (2), 713–723.
Séneca, J., Pjevac, P., Canarini, A., Herbold, C.W., Zioutis, C., Dietrich, M., Simon, E., Prommer, J., Bahn, M., Pötsch, E.M., Wagner, M., Wanek, W., Richter, A., 2020. Composition and activity of nitrifier communities in soil are unresponsive to elevated temperature and CO_2, but strongly affected by drought. ISME 14 (12), 3038–3053.
Shen, J., Jiao, N., Dai, M., Wang, H., Qiu, G., Chen, J., Li, H., Kao, S.-J., Yang, J.-Y., Cai, P., Zhou, K., Yang, W., Zhu, Y., Liu, Z., Chen, M., Zuo, Z., Gaye, B., Wiesner, M. G., Zhang, Y., 2020. Laterally transported particles from margins serve as a major carbon and energy source for dark ocean ecosystems. Geophys. Res. Lett. 47 (18) https://doi.org/10.1029/2020GL088971.
Shi, Q., Wallace, D., 2018. A 3-year time series of volatile organic iodocarbons in Bedford Basin, Nova Scotia: a northwestern Atlantic fjord. Ocean Sci. 14 (6), 1385–1403.
Smith, C.R., Deleo, F.C., Bernardino, A.F., Sweetman, A.K., Arbizu, P.M., 2008. Abyssal food limitation, ecosystem structure and climate change. Trends Ecol. Evol. 23 (9), 518–528.
Swan, B.K., Martinez-Garcia, M., Preston, C.M., Sczyrba, A., Woyke, T., Lamy, D., Reinthaler, T., Poulton, N.J., Masland, E.D.P., Gomez, M.L., Sieracki, M.E., DeLong, E.F., Herndl, G.J., Stepanauskas, R., 2011. Potential for chemolithoautotrophy among ubiquitous bacteria lineages in the dark ocean. Science 333 (6047), 1296–1300.
Tamburini, C., Boutrif, M., Garel, M., Colwell, R.R., Deming, J.W., 2013. Prokaryotic responses to hydrostatic pressure in the ocean—a review. Environ. Microbiol. 15 (5), 1262–1274.
Wältermann, M., Steinbüchel, A., 2005. Neutral lipid bodies in prokaryotes: recent insights into structure, formation, and relationship to eukaryotic lipid depots. J. Bacteriol. 187 (11), 3607.
Wang, Q., Garrity, G.M., Tiedje, J.M., Cole, J.R., 2007. Naive Bayesian classifier for rapid assignment of rRNA sequences into the new bacterial taxonomy. Appl. Environ. Microbiol. 73, 5261–5267.
Wasmund, K., Schreiber, L., Lloyd, K.G., Petersen, D.G., Schramm, A., Stepanauskas, R., Jørgensen, B.B., Adrian, L., 2014. Genome sequencing of a single cell of the widely distributed marine subsurface Dehalococcoidia, phylum Chloroflexi. ISME 8, 383.
Wu, F., Qing, H., Wan, G., 2001. Regeneration of N, P and Si near the sediment/water interface of lakes from Southwestern China Plateau. Water Res. 35 (5), 1334–1337.
Wu, X., Wu, L., Liu, Y., Zhang, P., Li, Q., Zhou, J., Hess, N.J., Hazen, T.C., Yang, W., Chakraborty, R., 2018. Microbial interactions with dissolved organic matter drive carbon dynamics and community succession'. Front. Microbiol. 9, 1234.
Wuchter, C., Abbas, B., Coolen, M.J.L., Herfort, L., van Bleijswijk, J., Timmers, P., Strous, M., Teira, E., Herndl, G.J., Middelburg, J.J., Schouten, S., Sinninghe Damste, J.S., 2006. Archaeal nitrification in the ocean. Proc. Natl. Acad. Sci. 103 (33), 12317–12322.
Yang, F., Mi, T., Chen, H., Yao, Q., 2019. Developing numeric nutrient criteria for the Yangtze River Estuary and adjacent waters in China. J. Hydrol. 579, 124188. https://doi.org/10.1016/j.jhydrol.2019.124188.
Zhang, S., Hu, Z., Wang, H., 2019. Metagenomic analysis exhibited the co-metabolism of polycyclic aromatic hydrocarbons by bacterial community from estuarine sediment. Environ. Int. 129, 308–319.
Zhang, Y., Xiao, W., Jiao, N., 2016. Linking biochemical properties of particles to particle-attached and free-living bacterial community structure along the particle

density gradient from freshwater to open ocean. J. Geophys. Res. Biogeosci. 121 (8), 2261–2274.
Zhang, Y., Qin, W., Hou, L., Zakem, E.J., Wan, X., Zhao, Z., Liu, L., Hunt, K.A., Jiao, N., Kao, S.-J., Tang, K., Xie, X., Shen, J., Li, Y., Chen, M., Dai, X., Liu, C., Deng, W., Dai, M., Ingalls, A.E., Stahl, D., Herndl, G.J., 2020. Nitrifier adaptation to low energy flux controls inventory of reduced nitrogen in the dark ocean. Proc. Natl. Acad. Sci. 117 (9), 4823–4830.
Zheng, Q., Chen, Q., Cai, R., He, C., Guo, W., Wang, Y., Shi, Q., Chen, C., Jiao, N., 2019. Molecular characteristics of microbially mediated transformations of Synechococcus-derived dissolved organic matter as revealed by incubation experiments. Environ. Microbiol. 21 (7), 2533–2543.